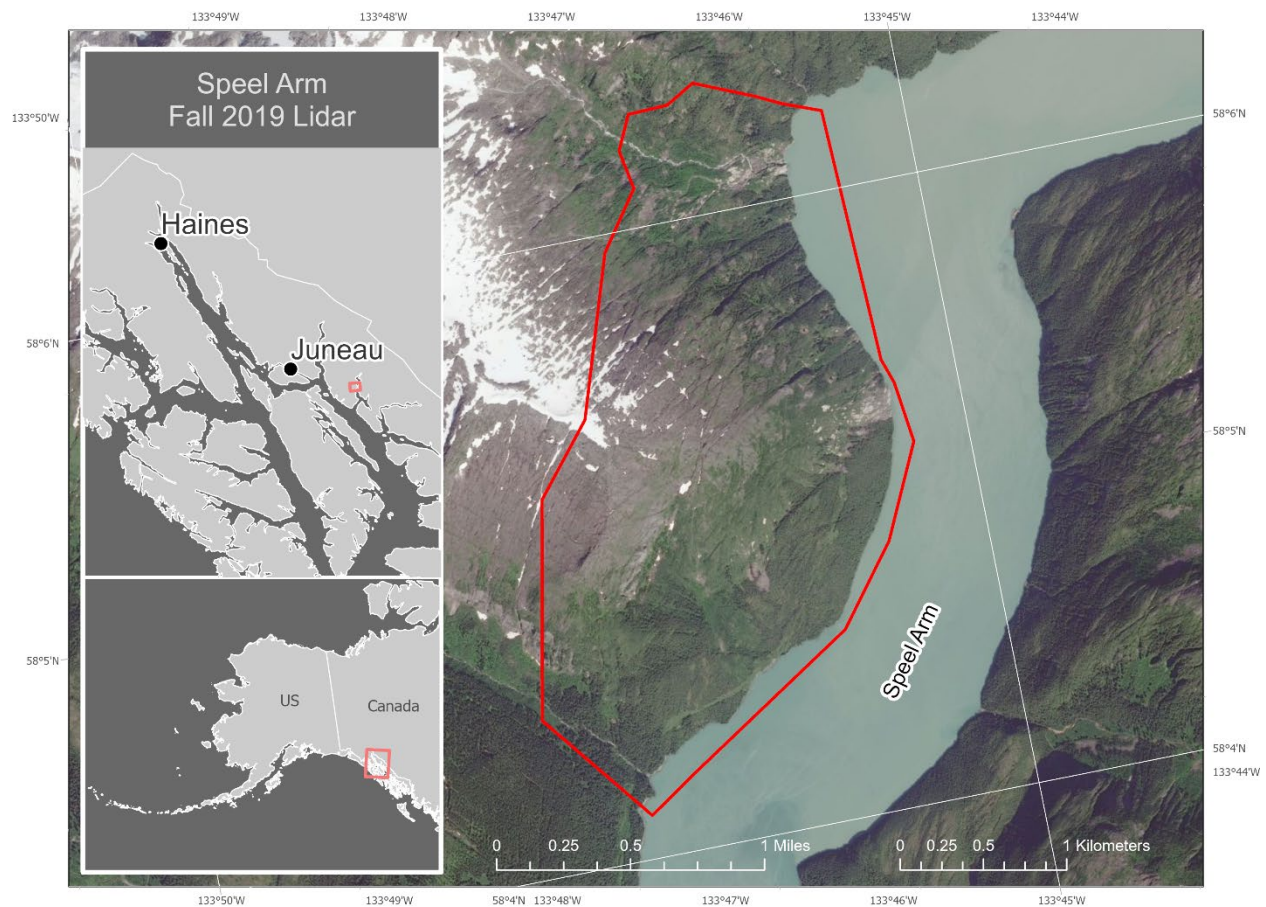


LIDAR-DERIVED ELEVATION DATA FOR SPEEL ARM, SOUTHEAST ALASKA, COLLECTED SEPTEMBER 7, 2019

Katreen Wikstrom Jones and Gabriel J. Wolken

Raw Data File 2021-11



Location map of survey area with orthometric image.

This report has not been reviewed for technical content or
for conformity to the editorial standards of DGGs.

2022
STATE OF ALASKA
DEPARTMENT OF NATURAL RESOURCES
DIVISION OF GEOLOGICAL & GEOPHYSICAL SURVEYS



STATE OF ALASKA

Mike Dunleavy, Governor

DEPARTMENT OF NATURAL RESOURCES

Corri A. Feige, Commissioner

DIVISION OF GEOLOGICAL & GEOPHYSICAL SURVEYS

David LePain, State Geologist & Director

Publications produced by the Division of Geological & Geophysical Surveys are available to download from the DGGS website (dggs.alaska.gov). Publications on hard-copy or digital media can be examined or purchased in the Fairbanks office:

Alaska Division of Geological & Geophysical Surveys (DGGS)

3354 College Road | Fairbanks, Alaska 99709-3707

Phone: 907.451.5010 | Fax 907.451.5050

dggspubs@alaska.gov | dggs.alaska.gov

DGGS publications are also available at:

Alaska State Library, Historical
Collections & Talking Book Center
395 Whittier Street
Juneau, Alaska 99801

Alaska Resource Library and
Information Services (ARLIS)
3150 C Street, Suite 100
Anchorage, Alaska 99503

Suggested citation:

Wikstrom Jones, Katreen, and Wolken, G.J., 2022, Lidar-derived elevation data for Speel Arm, Southeast Alaska, collected September 7, 2019: Alaska Division of Geological & Geophysical Surveys Raw Data File 2021-11, 8 p.

<https://doi.org/10.14509/30730>



LIDAR-DERIVED ELEVATION DATA FOR SPEEL ARM, SOUTHEAST ALASKA, COLLECTED SEPTEMBER 7, 2019

Katreen Wikstrom Jones¹ and Gabriel J. Wolken¹

INTRODUCTION

The Alaska Division of Geological & Geophysical Surveys (DGGS) used aerial lidar to produce a classified point cloud, digital surface model (DSM), digital terrain model (DTM), and intensity model of a mountain slope adjacent to Speel Arm near Port Snettisham, Southeast Alaska, during near snow-free ground conditions on September 7, 2019. The survey provides snow-free surface elevations for deriving snow depth distribution models with repeat surveys during snow-covered conditions. Aerial lidar and ground control data were collected on September 7, 2019, and subsequently processed in a suite of geospatial processing software. This data collection is released as a Raw Data File with an open end-user license. All files are available here:

<https://doi.org/10.14509/30703>.

LIST OF DELIVERABLES

Classified Points

DSM and DTM

Intensity Image

Metadata

MISSION PLAN

Aerial Lidar Survey Details

DGGS used a Riegl VUX1-LR laser scanner integrated with a global navigation satellite system (GNSS) and Northrop Grumman LN-200C inertial measurement unit (IMU). The lidar integration system was designed by Phoenix LiDAR Systems. The sensor can collect up to 820,000 points per second at a range of up to 150 m. The scanner operated with a pulse refresh rate of 50,000 pulses per second in the alpine areas and 400,000 pulses per second over forested areas at a scan rate between 80 and 220 lines per second. We used a Bell 206 JetRanger aircraft to survey from an elevation of ~130 m above ground level, at a ground speed of approximately 30 m/s, and with a scan angle set from 80 to 280 degrees. The total surveyed area covers ~6 km² (fig. 1).

Weather Conditions and Flight Times

We flew the aerial survey on September 7, 2019, with departure at 3:20 pm from Speel Arm Balcony weather station and landed back at the same location at 4:45 pm (fig. 1). The weather throughout the survey was clear with no wind.

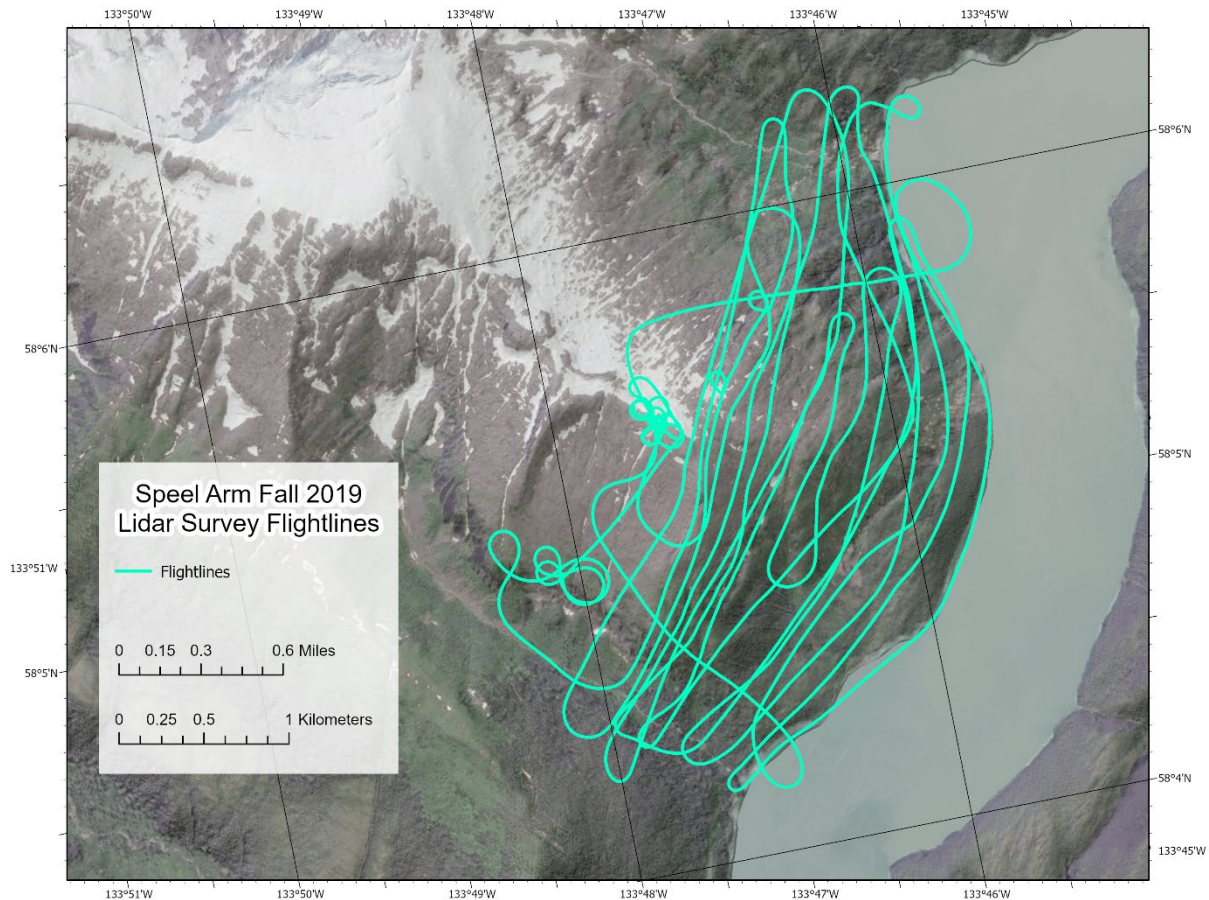


Figure 1. Project flightlines.

PROCESSING REPORT

Lidar Dataset Processing

We processed point data in SDCimport software for initial filtering and multiple-time-around (MTA) disambiguation. MTA errors, corrected in this process, are the result of ambiguous interpretations of received pulse time intervals and occur more frequently with higher pulse refresh rates. We processed Inertial Measurement Unit (IMU) and Global Navigation Satellite System (GNSS) data in Inertial Explorer and we used Spatial Explorer software to integrate flightline information with the point cloud. We calibrated the point data at an incrementally precise scale of sensor movement and behavior, incorporating sensor velocity, roll, pitch, and yaw fluctuations throughout the survey.

We created macros in Terrasolid software and classified points in accordance with American Society for Photogrammetry and Remote Sensing (ASPRS) 2014 guidelines. We gave careful attention to the interpolation of the project's ground surface to compensate for inconsistent penetration through low vegetation as a function of the scan angle. Once classified, we applied a geometric transformation and converted the points from ellipsoidal heights to GEOID12B (Alaska) orthometric heights.

We used ArcMap to derive raster products from the point cloud. The DSM was interpolated from maximum return values from the ground, vegetation and building classes using a binning method. The DTM was interpolated from all ground class returns also using a binning method and minimum values. In ArcMap, we produced an intensity image using closest-to-mean binning.

Classified Point Cloud

Classified point cloud data are provided in compressed LAZ format. Data are classified in accordance with ASPRS 2014 guidelines and contain return and intensity information. The average pulse spacing is 3 cm and the average density is 48.5 pts/m².

Digital Surface Model

The DSM represents surface elevations including heights of vegetation, buildings, powerlines, etc. The DSM is a single band, 32-bit GeoTIFF file of 50-centimeter resolution. No Data value is set to -3.40282306074e+38 (32-bit, floating-point minimum).

Digital Terrain Model

The DTM represents surface elevations of ground surfaces, excluding vegetation, bridges, buildings, etc. The DTM is a single-band, 32-bit float GeoTIFF file of 50-centimeter resolution. No Data value is set to -3.40282306074e+38.

Lidar Intensity Image

The lidar intensity image describes the relative amplitude of reflected signals contributing to the point cloud. Intensity is largely a function of scanned object reflectance in relation to the signal frequency, is dependent on ambient conditions, and is not necessarily consistent between separate scans. The intensity image is a single-band, 32-bit float GeoTIFF file of 50-centimeter resolution. No Data value is set to -3.40282306074e+38.

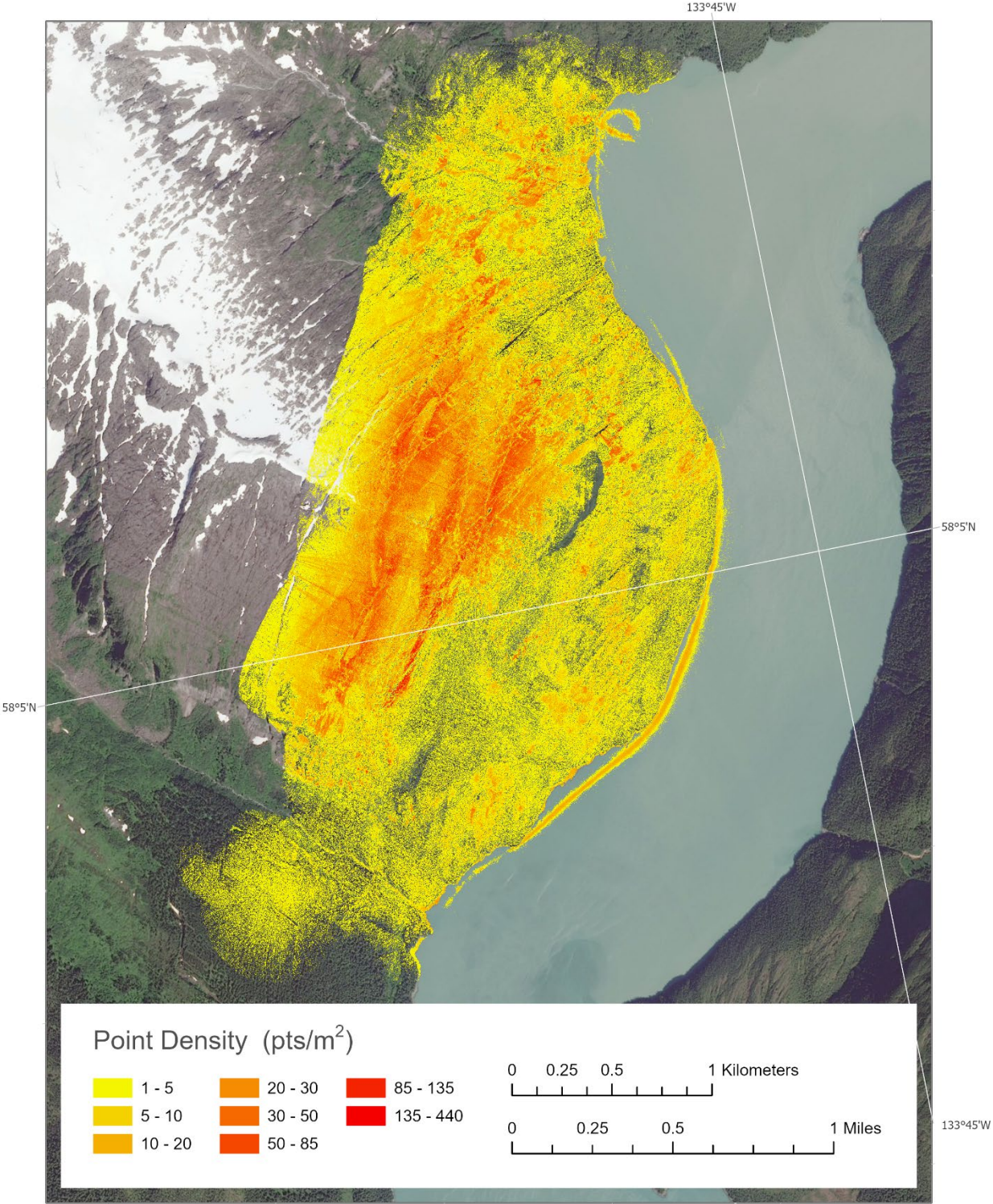


Figure 2. Ground point density for the survey displayed as a 1-meter raster.

SURVEY REPORT

Ground Survey Details

We collected ground control and check points on September 7, 2019. We deployed a Trimble R7 GNSS receiver with Zephyr-2 antenna near the Speel Arm Balcony weather station. It provided a base station occupation and real-time kinematic (RTK) corrections to points that we surveyed with a rover Trimble R8-4 GNSS receiver (internal antenna). We collected a total of 51 ground control points and check points to use for calibration and to assess the vertical accuracy of the point cloud. All points were collected on bare earth or paved surfaces.

Coordinate System and Datum

We processed and deliver all data in NAD83 (2011) UTM8N and vertical datum NAVD88 GEOID12B.

Horizontal Accuracy

We did not measure horizontal accuracy for this collection.

Vertical Accuracy

We measured a mean offset of -21.3 cm between 39 control points and the point cloud (appendix 1). We reduced this offset to -0.3 cm by performing a vertical transformation of the lidar point data. We used 12 check points to determine the non-vegetated vertical accuracy (NVA) of the point cloud ground class using a Triangulated Irregular Network (TIN) approach. We calculated the project NVA to have a root mean square error (RMSE) of 18.6 cm (appendix 2). We evaluated the relative accuracy for this dataset as the interswath overlap consistency and measured it at a 1.8 cm RMSE.

Data Consistency and Completeness

This data release is complete, and there was no over collect except for aircraft turns that were eliminated from the dataset. The data quality is consistent throughout the survey, apart from a sliver-shaped area in the center of the survey area where lack of overlap between the flightlines resulted in a gap in the lidar coverage. When we built the DSM and DTM in ArcGIS, we interpolated this area using Natural Neighbor void filling.

ACKNOWLEDGMENTS

These data products were funded by U.S. Geological Survey, Alaska Electric Light & Power and the State of Alaska and collected and processed by DGGS. We thank Coastal Helicopters for their aviation expertise and contribution to these data products. The views and conclusions contained in this document are those of the authors and should not be interpreted as necessarily representing the official policies, either expressed or implied, of the U.S. Government.

APPENDIX 1: GROUND CONTROL POINTS

GCP	Easting (m)	Northing (m)	Known Z (m)	Laser Z (m)	Dz (m)
1	571457.94	6439252	1044.936	1044.95	0.014
2	571455.01	6439264	1045.438	1045.19	-0.248
3	571458.26	6439275	1046.289	1046.33	0.041
4	571468.42	6439288	1048.091	1047.85	-0.241
5	571480.89	6439279	1046.839	1046.61	-0.229
6	571487.08	6439274	1046.34	1045.85	-0.49
7	571494.05	6439272	1044.625	1044.51	-0.115
8	571492.24	6439255	1043.56	1043.74	0.18
9	571485.45	6439238	1042.844	1042.55	-0.294
10	571482.17	6439231	1041.749	1041.79	0.041
11	571476.89	6439215	1041.6	1041.5	-0.1
12	571485.47	6439207	1041.032	1040.88	-0.152
13	571487.66	6439203	1041.409	1040.76	-0.649
14	571496.21	6439202	1041.936	1041.58	-0.356
15	571505.21	6439214	1043.035	1042.65	-0.385
16	571509.97	6439215	1043.156	1042.54	-0.616
17	571508.23	6439193	1038.898	1038.87	-0.028
18	571504.47	6439177	1036.209	1035.93	-0.279
19	571514.54	6439174	1037.276	1037.3	0.024
20	571524.33	6439169	1034.697	1034.5	-0.197
21	571534.47	6439164	1032.061	1031.48	-0.581
22	571533.59	6439153	1029.723	1029.37	-0.353
23	571527.11	6439145	1026.423	1026.44	0.017
24	571542.31	6439132	1022.501	1022.09	-0.411
25	571537.03	6439127	1020.674	1020.5	-0.174
26	571539.72	6439117	1019.828	1019.65	-0.178
27	571534.74	6439111	1019.543	1019.17	-0.373
28	571546.76	6439122	1019.957	1019.58	-0.377
29	571549.99	6439127	1020.183	1019.94	-0.243
30	571553.59	6439129	1019.238	1019.28	0.042

31	571552.7	6439141	1020.573	1020.35	-0.223
32	571558.33	6439160	1019.564	1019.49	-0.074
33	571559.14	6439166	1019.914	1019.11	-0.804
34	571559.4	6439180	1021.447	1021.24	-0.207
35	571542.7	6439183	1031.745	1031.62	-0.125
36	571538.88	6439181	1032.628	1032.56	-0.068
37	571527.38	6439186	1035.946	1035.93	-0.016
38	571535.98	6439188	1034.63	1034.58	-0.05
39	571539.39	6439204	1034.071	1034.05	-0.021
Average dz (m)	-0.213				
Minimum dz (m)	-0.804				
Maximum dz (m)	0.18				
Average magnitude error (m)	0.231				
Root mean square error (m)	0.303				
Standard deviation (m)	0.218				

APPENDIX 2: CHECK POINTS

Check Point	Easting (m)	Northing (m)	Known Z (m)	Laser Z (m)	Dz (m)
2	571465	6439281	1047.703	1047.58	-0.123
3	571497.3	6439263	1043.394	1043.73	0.336
4	571480.8	6439223	1042.433	1042.35	-0.083
5	571501.8	6439208	1042.573	1042.17	-0.403
6	571505.2	6439188	1038.412	1038.26	-0.152
7	571521.1	6439161	1034.593	1034.69	0.097
8	571525.4	6439140	1025.994	1025.91	-0.084
9	571548.6	6439117	1018.97	1019.05	0.08
10	571554.7	6439159	1019.926	1019.98	0.054
11	571563.6	6439188	1019.465	1019.54	0.075

12	571537.2	6439198	1034.401	1034.57	0.169
Average dz (m)	-0.003				
Minimum dz (m)	-0.403				
Maximum dz (m)	0.336				
Average magnitude error (m)	0.151				
Root mean square error (m)	0.186				
Standard deviation (m)	0.195				